2nd URSI AT-RASC, Gran Canaria, 28 May – 1 June 2018

Wearable breathing sensor based on Modulated Frequency Selective Surfaces

A.Lazaro, S.Milici, R.Villarino, D.Girbau
Universitat Rovira i Virgili, Av.Paisos Catalans, 26, 43007, Tarragona, Spain, antonioramon.lazaro@urv.cat

Abstract

This work describes a wearable wireless breathing sensor based on modulated frequency selective surfaces (FSS) at 2.45 GHz ISM band. The breathing information is obtained measuring the variation of the airflow temperature during the breathing. The temperature sensor consists of a negative temperature coefficient resistor, which is to be placed close to the nose. The variation of the temperature changes the oscillation frequency of a low-frequency oscillator which modulates the radar cross section of the FSS. The FSS is composed by dipoles printed on a flexible substrate. The dipoles response can be modulated by changing the polarization of the varactor diodes. The communication with the reader is by backscattering. Therefore, it is not required a transmitter to send the information. A low-power prototype is designed allowing a long battery life time. A real-time algorithm implemented in the reader allows the measuring of real-time breathing rate and detection of apneas. Read ranges of 3 m for a prototype of FSS located in a headband have been achieved.

1. Introduction

A great growing of wearable devices is expected in the next years [1]. One of the fields where users are showing an increasing interest is in their use for health monitoring. One research direction is focused on the development of devices compatible with clothes known as E-textile wearables [1]. In this sense, efforts to develop antennas for Wireless Body Networks (WBAN) have been proposed [2]. Most of them are equipped with powerful microcontrollers and the data transmission is performed using Bluetooth Low Energy (BLE). However, one of the points that must be improved is the battery lifetime, especially for continuous real-time monitoring applications–because an important part of the power is required for transmission. Therefore, in order to increase the battery lifetime, to reduce the size of the batteries or the number of recharges, advanced designs in which the data communication is based on backscattering communication can be useful.

In previous works, the authors have shown that modulated frequency selective surfaces can be used due to its great bandwidth for FMCW radar transponders [3] and on-body communications based on backscattering [4]-[7]. Even using a simple FSS composed by loaded dipoles with switching elements, read-ranges up to 3 m at 2.45 GHz ISM band can be achieved [4]. In order to reduce the power consumption, reverse-biased varactor diodes can be employed as switching elements. The varactors are feed with a low-power oscillator (timer 555 or NAND gates based oscillator) whose oscillation frequency (f_m) can be used for identification or by sensing purposes. Following the analysis described in [3], the received signal at the modulation frequency offset from the illuminating carrier is proportional to the differential radar cross section between the two diode states. The magnitude of differential RCS increases with the number of FSS elements. Therefore, when the surface of the FSS is increased the effect of the losses due to the proximity of the body is reduced whereas the great bandwidth allows to minimize the effects of the detuning due to the variability of the dielectric properties between persons or body locations. In [6], the authors studied the improvements in received power by using tag diversity. The use of modulated FSS to transmit the same data located at different parts of the body or the use of different polarizations improve the data communication in front of a multipath and body blocking effects. The feasibility of printing modulated FSS on different substrates opens new expectations in wearable applications. A proof of concept of wearable breathing sensor based on FSS is described in Section 2. Some experimental results are summarized in section 3. Finally, some conclusions and future lines are depicted in section 4.

2. System description

Figure 1 shows the block diagram of the different parts of the system to measure the breathing rate. It is composed of a negative temperature coefficient resistor (NTC) installed close to the nose to sense the airflow temperature variation. The NTC model NB20R00105JBA from AVX with nominal resistance of 1 MΩ and the Steinhart–Hart parameter β=4400K has been used. The resistance controls a low-power oscillator composed by two inverters (NAND gates). The oscillation frequency is given by f_m=0.455/RC, where R is the NTC resistance and C is the capacitor of the oscillator. The afore mentioned oscillator draws 40 μA at 3V; this means that the lifetime of a standard 330 mAh coin-battery leads to more than one year. According to the circuit, a variation ΔT in the

temperature is translated to a variation on the oscillation frequency Δf_m given by:

$$\frac{\Delta f_m}{f_m} \approx \frac{\beta}{T} \cdot \frac{\Delta T}{T} \quad (1)$$

The output of the oscillator is used to bias the varactors that load the dipoles of the FSS. In the prototype, low-cost silicon varactors from Skyworks SMV1247-079LF are used. The advantages of using these as switching devices in front of the PIN diodes [3] is that they can be reverse-biased between 0V (high capacitance state) and -3V (low capacitance sate), reducing considerably their power consumption. The FSS has been built using a 100 µm thick Ultralam® 3850 flexible substrate (see Figure 2). The feed lines are orthogonal to the dipole direction to avoid interference in the backscattered field. In order to block the RF signal, 10kΩ 0605 SMD resistors are connected at the end of the arms of the dipole. The dipole length is adjusted to resonate at about 2.45GHz. Its length and width are 25 mm and 2 mm, respectively, and the dipoles are spaced among them 10.24 mm. A photograph of the prototype is shown in Fig.3.

When a wave generated by the reader illuminates the surface of the FSS, a part of the power is backscattered and demodulated by the reader. The backscattered field is proportional to the differential radar cross section [3] that depends on the reflection coefficients between the two diode states. The result is that the backscattered field changes at a rate of the modulation frequency that depends on the temperature of the airflow. The modulation frequency can be measured at baseband after a down conversion. It can be obtained from the Fourier transform of the discretized signal at the output of an A/D converter. The chirp Z-transform (CZT) algorithm [8], and a Hamming window are used to achieve the required frequency resolution. A custom reader has been designed to this purpose using cost components [6]. It uses a synthesizer KSN-2450A-119+ from Minicircuits to generate the transmitting tone, that is amplified by a Minicircuits GAL-84+ driver amplifier up to 18 dBm and also serves as local oscillator for the mixer (Minicircuits LRMS-3J) that downconverts the amplified received signal. After a baseband amplifier based on two stages of inverter operational amplifiers, the baseband signal is sampled by a PC sound card used as a low-cost A/D.

The signal processing applied to the sampled signal is depicted in Figure 4. The average temperature of the sensor depends on the distance to the body and to the nose. Therefore, the breathing signal x[n] is obtained after blocking the dc component. To this end a first moving averaging filter is used to dynamically estimate the average modulation frequency and it is subtracted to the measured f_m. A second moving averaging filter is applied to x[n] to remove the noise. After denoising the breathing signal, a peak detector is used to find the maximum value of y[n]. The breathing interval is obtained from the difference from two consecutive peaks. Details of the algorithm are given in [7]. An apnoea is considered to happen if the breathing interval is higher than 10 seconds. Note that a recursive implementation of the filters is done, therefore a real-time breathing measurement is performed.

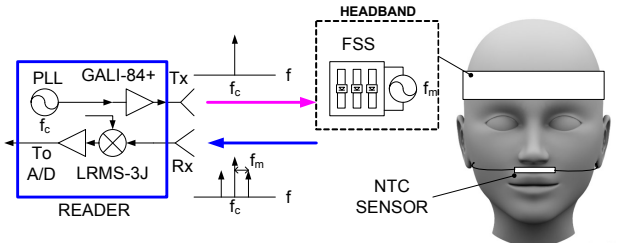

Figure 1. Block diagram of the system, including the reader and the transponder.

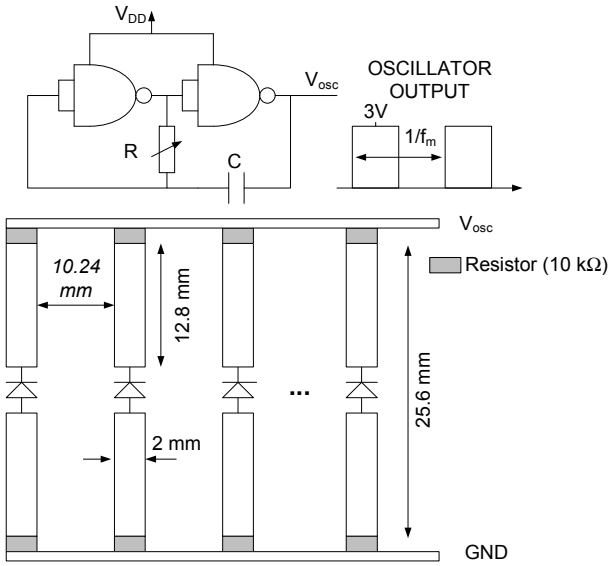

Figure 2. Schema of a FSS loaded with varactors connected to the two-inverter oscillator controlled by the NTC resistance (R).

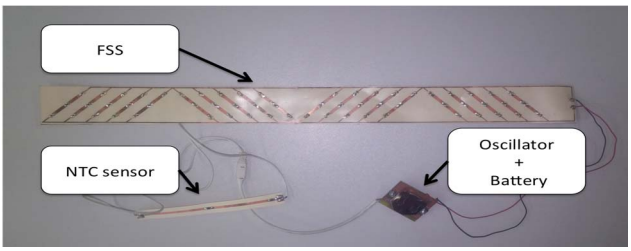

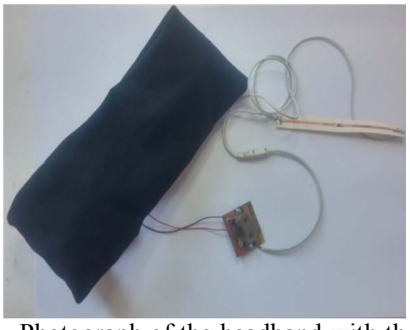

Figure 3. Photograph of the headband with the FSS and the NTC sensor and the oscillator.

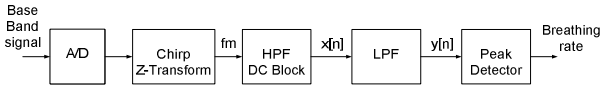

Figure 4. Block diagram of the signal processing for breathing rate measurement.

3. Experimental results

Figure 5 shows the received level as a function of the frequency of a modulated FSS, placed on the arm, at a distance of 1 m. It is observed that the received level increases with the number of elements (dipoles) of the FSS and the response is nearly flat in a bandwidth of more than 1 GHz. The conclusions obtained are very similar when the FSS is located in other parts of the body or when different phantoms are used [4,5]. Therefore, these results allow to use the FSS for communications in wearable applications [6].

Figure 6 shows the measurement performed with a spectrum analyzer when a FSS of 7 elements located at the arm is illuminated injecting a 20 dBm tone at 2.45 GHz from a generator. The central peak at the CW frequency is due to the coupling between the transmit and receive antennas and remains nearly constant with distance. The sideband peaks at the modulating frequency (5 kHz in this example) depend on the distance. It can be seen that more than 4 m can be reached. Figure 7 shows the received power as function of the distance. For distances under 1.5 m the propagation can be considered in Line-Of-Sight (LOS), however for higher distances the antennas also illuminate the surrounding objects and multipath interference appears, which must be taken into account in order to check the correct working of the sensor. A heat gun is pointed to the sensor close to the other sensor wired used to measure the temperature. Good agreement is obtained between the measurements performed (modulation frequency as a function of temperature) and the ideal model derived from the oscillation frequency) produced by the variation of the resistance as a function of the temperature given by the thermistor manufacturer. Figure 9 shows the histogram obtained from the recorded of the samples at the output of the reader at room temperature (assumed constant). The resolution is better than 0.05ºC. This is due to the amplification gain of the factor β/T that is very large in (1). Therefore, resolutions on the order of 1-2 Hz in the measurement of the modulation frequency produce resolutions around of 0.01-0.02ºC in temperature. Figure 9 shows an example of breathing measurement. Figure 9a shows the frequency modulation measurement obtained from the CZT at the reader. The cyclic variation is due to the expiration (increase of temperature due to the hot air) and inspiration (cooling due to the input air) periods. Figure 9b shows the temperature variation and figure 9c the real-time breathing rate estimated from the peak detection algorithm. It can be observed an apnea when the temperature decreases since the airflow stops.

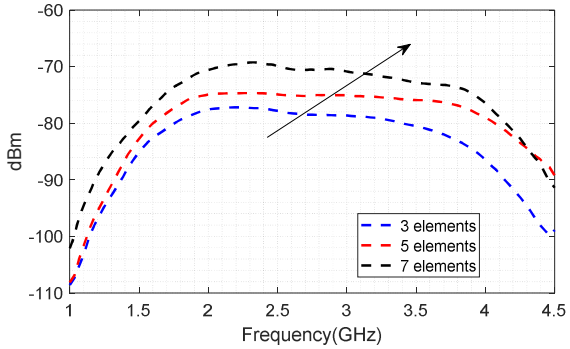

Figure 5. Measured received power as function of illumination carrier frequency.

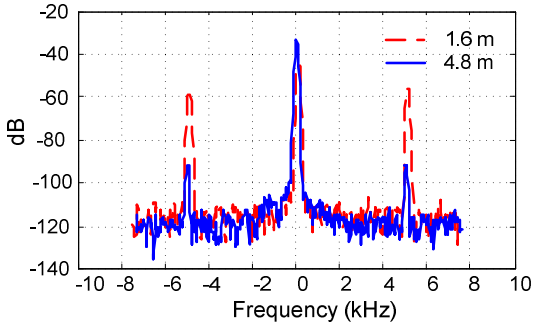

Figure 6. Comparison of the spectrum obtained at the output baseband of the reader for 1.6 m and 4.8 m.

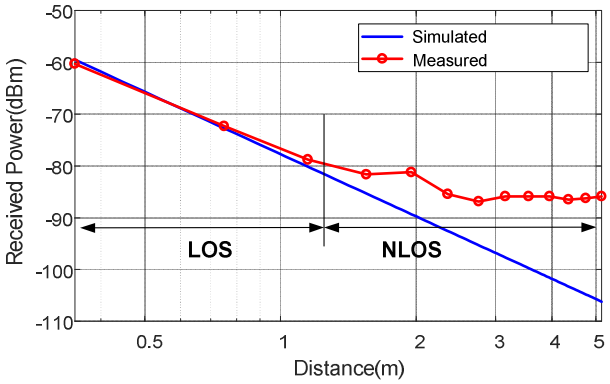

Figure 7. Measured received power as function of read distance and comparison with ideal free space model.

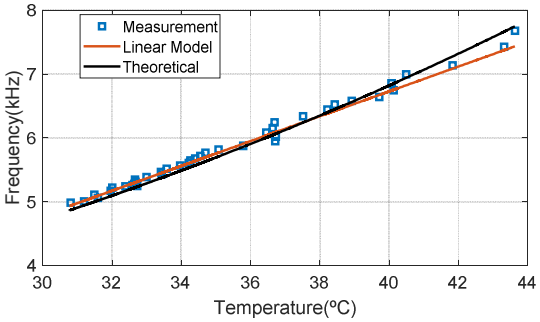

Figure 8. Measured modulation frequency (f_m) as a function of the thermistor temperature. Comparison with the linear regression model and theoretical model.

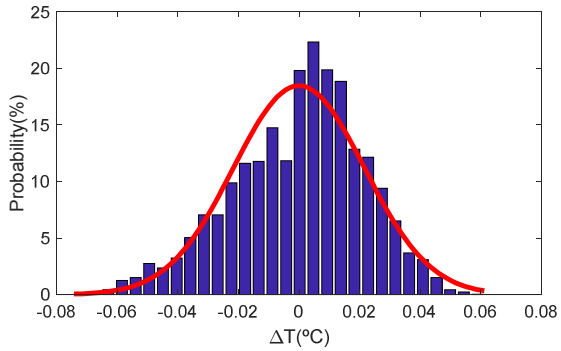

Figure 9. Histogram and fitted probability density of the measured temperature at room temperature.

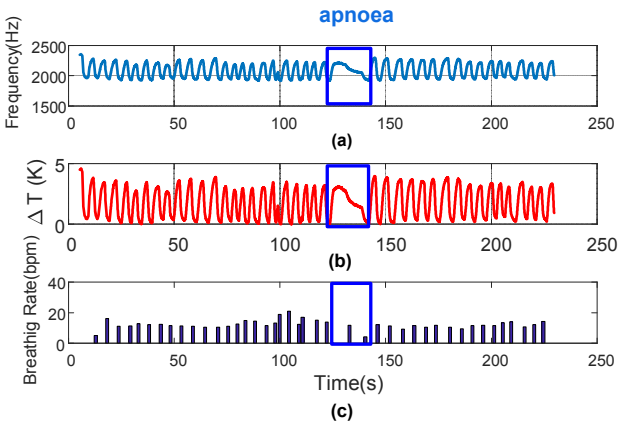

Figure 10. Measured modulation frequency (a), temperature variation (b) and breathing rate in bpm (c) as a function of the time.

4. Conclusions

A system for wireless breath monitoring and apnoea detection has been presented. The communication between the transponder and the reader has been performed by the backscattering technique. The radar cross section of the FSS-based transponder is modulated using low-cost reverse-biased varactors. Therefore, the power consumption of the semi-passive FSS is smaller than other active alternatives based on RF transmitters. The varactors are driven by an oscillator and the frequency is controlled by a thermistor placed close to the nose cavities which sense the airflow temperature during respiration. In order to increase robustness in front of fadings due to Non-Line-Of-Sight (NLOS) situations, the transponder contains several FSS's with different directions and it is integrated in a headband located around the head. A custom reader has also been developed using commercial components. Read ranges up to 3 m are typically obtained with the proof-of-concept prototype in indoor environments. A real-time algorithm based on determining the interval between respiration peaks to measure the breathing rate and detect the apnoea intervals is used. The low power consumption enables long-term recording sessions of apnoea monitoring for screening applications at home.

5. Acknowledgements

This work was supported by the Spanish Government Project TEC2015-67883-R, H2020 Grant Agreement 645771–EMERGENT, MiMed COST Action TD1301.

6. References

1. N. R. Rishani, R. M. Shubair and G. Aldabbagh, "On the design of wearable and epidermal antennas for emerging medical applications," 2017 Sensors Networks Smart and Emerging Technologies (SENSET), Lebanon, 2017, pp. 1-4. doi: 10.1109/SENSET.2017.8125046

2. S. Seneviratne *et al*., "A Survey of Wearable Devices and Challenges," in *IEEE Communications Surveys & Tutorials*, vol. 19, no. 4, pp. 2573-2620, Fourthquarter 2017. doi: 10.1109/COMST.2017.2731979

3. A. Lazaro, J. Lorenzo, R. Villarino, and D. Girbau, "Backscatter Transponder Based on Frequency Selective Surface for FMCW Radar Applications," Radioengineering, vol. 23, no. 2, Jun. 2014.

4.J. Lorenzo, A. Lazaro, R. Villarino, and D. Girbau, "Modulated Frequency Selective Surfaces for wearable RFID and sensor applications," IEEE Trans. Antennas Propag., vol. PP, no. 99, pp. 1–1, 2016. doi: 10.1109/TAP.2016.2596798

5. J. Lorenzo, A. Lazaro, D. Girbau, R. Villarino, E. Gil, "Analysis of on-Body Transponders Based on Frequency Selective Surfaces," Progress In Electromagnetics Research, Vol. 157, pp.133-143, 2016. doi:10.2528/PIER16082501

6. J. Lorenzo, A. Lazaro, R. Villarino and D. Girbau, "Diversity Study of a Frequency Selective Surface Transponder for Wearable Applications," in IEEE Transactions on Antennas and Propagation, vol. 65, no. 5, pp.2701-2706,May 2017.
doi: 10.1109/TAP.2017.2681435

7. S. Milici, J. Lorenzo, A. Lazaro, R. Villarino and D. Girbau, "Wireless Breathing Sensor Based on Wearable Modulated Frequency Selective Surface," in IEEE Sensors Journal, vol. 17, no. 5, pp. 1285-1292, March1, 1 2017. doi: 10.1109/JSEN.2016.2645766

8. L. Rabiner, R. Schafer, and C. Rader, "The chirp z-transform algorithm," IEEE Trans. Audio Electroacoustics, vol. 17, no. 2, pp. 86–92, 1969. doi: 10.1109/TAU.1969.1162034